Relaxation Dynamics of Hydration Water at Activated Silica Interfaces in High-Performance Elastomer Composites

Johann G. Meier,[†,§] Juliane Fritzsche,[†] Laurent Guy,[‡] Yves Bomal,[‡] and Manfred Klüppel*,[†]

Deutsches Institut für Kautschuktechnologie e.V., Eupener Str. 33, D-30519 Hannover, Germany; Rhodia Recherche & Technologie, 15 rue Pierre Pays, BP 52, F-69660 Collonges-au-Mont-d'Or, France; and Departamento de Materiales, Instituto Tecnológico de Aragón, Calle María de Luna 8, E-50018 Zaragoza, Spain

Received September 2, 2008; Revised Manuscript Received January 13, 2009

ABSTRACT: The dynamics of hydration water at the silica interface of elastomer (S-SBR) composites filled with various types of silica with and without activation by silane is investigated by broadband dielectric spectroscopy. This gives some new insight into the mechanisms of silane coupling and polymer−filler interaction in silica-filled high-performance elastomers. Depending on the hydration level of the silica, water islands or complete coverage of the silica surface with at least one monolayer of water are identified by the dielectric response. The observed two low-temperature relaxation transitions are shown to be related to fluctuations of physically adsorbed water (SP1) and of hydroxyl groups (SP2), respectively, differing in relaxation strength and activation energy. The relaxation strength of the main peak SP1 decreases with silanization, indicating that, due to hydrophobization of the silica surface, part of the adsorbed water migrates into the rubber matrix. At low surface coverage, below one monolayer of water, the activation energy of both relaxation transitions is found to increase with the hydration level due to an increasing mean number of interacting hydrogen bonds in the merging water islands (SP1) and a rising number of water−hydroxyl interactions (SP2). Above one monolayer of water, the activation energy becomes almost independent of hydration level. For nonactivated silica composites (without silane), the activation energy of the main peak SP1 is close to the value 0.6 eV, also observed in ice. Modification of the silica interface by silane increases the activation energy up to about 0.7 eV, indicating that hydrophobization and chemical coupling of the polymer chains to the silica surface reduces the mobility of the hydration water. This opens the possibility to assess and predict the coupling strength of the polymer chains to the silica surface by measuring the activation energy of the hydration water of the composites.

Introduction

Reinforcement of elastomers by activated silica fillers plays an important role in improving the mechanical potential of rubber goods. In particular, the rolling resistance and wet traction properties of tires could be improved significantly by the incorporation of precipitated silica in tire treads delivering the so-called green tires.[1] This new generation of high-performance tires was developed by referring to an in situ activation of the silica surface by multifunctional silanes, allowing for an effective dispersion of the nanoparticles as well as a chemical coupling of the polymer chains to the silica surface. By this technique reasonable wear properties of the tire tread could be realized. Nevertheless, a further optimization of the green tire performance by tailor-made polymer−filler couplings is of high technological interest.

Despite numerous studies devoted to these materials, the reinforcement mechanism of the silica-filled rubbers has not been clarified to such an extent as that of carbon black-filled rubbers where it has been ascribed to strong physical adsorption of polymer chains onto the carbon black surface often attributed as bound rubber. Contrary to carbon black, the interaction between hydrophilic silica surfaces and hydrophobic polymer chains is not attractive due to the different polarities. However, removal of all the hydroxyl groups by treating silica with e.g. dimethyldichlorosilane or hexamethyldisilane renders the silica hydrophobic, but such silicas do not show sufficient reinforcing properties and behave more like inert fillers with poor abrasion resistance, etc., evidencing the need of silanol groups for the formation of the reinforcing filler network. Moreover, several studies have demonstrated that there is even a higher amount of bound rubber on silicas without than with hydrophobic surface modification.[2−7] This seems to contradict the expected repulsive behavior due to the different chemical nature of silica and hydrocarbon chains, but it is probably just an indication for the insufficiency of bound rubber measurements to predict the polymer−filler interaction strength. A possible explanation for such unexpected results can be found in the high stability of the filler network with strong hydrogen bonds between the silica particles. This can imply that part of the polymer chains are occluded by stable filler clusters that are not resolved by the solvent. Hence, the occluded polymer chains are counted as additional bound rubber though they are not directly bounded to the filler surface.

The interaction of glass-forming polymers with solid surfaces of different anchoring conditions has been studied extensively on model systems of thin films deposited onto different substrates studied by elipsometry, dielectric spectroscopy, NMR, etc. In the case of attractive walls, an increase of the glass transition temperature is observed with decreasing film thickness.[8,9] A pronounced reduction of the glass transition temperature has been observed in confined geometries, e.g., various porous media,[10] or in the case of unsupported, free-standing thin films[11] and supported thin films by noncompatible substrates.[8,9] Long and Lequeux[12] proposed a strongly heterogeneous dynamics of the glass transition and described it by a percolation transition of nanoscopic domains of slow dynamics. This model allows for an explanation of the variation of the glass transition temperature of thin films for both attractive and

* Corresponding author: e-mail Manfred.Klueppel@DIKautschuk.de; Fax + +49-511-8386826.
[†] Deutsches Institut für Kautschuktechnologie e.V.
[‡] Rhodia Recherche & Technologie.
[§] Instituto Tecnológico de Aragón.

10.1021/ma802002s CCC: $40.75
Published on Web 02/20/2009

Table 1. Water and Ignition Loss of the Used Silicas and Silanol Groups per nm² Silica Surface Calculated from That Data[a]

silica	moisture (%), 2 h at 105 °C (ISO 787-2)	loss ignition (%) at 1000 °C (ISO 3262-14)	specific surface (N_2adsorption), m^2/g	Si−OH per nm^2	main pore diameter d_{max}, nm	porous distribution width parameter
Z1115MP	6.5	10.0	110	21.3	58	0.65
Z1165MP	6.1	9.7	160	15.1	30	0.52
Siloa72X	3.1	5.06	175	7.6	27	0.48
Zeosil PREMIUM 200MP	5.4	8.10	216	8.4	21	1.54
ZHRS 1200MP	6.7	10.0	195	11.3	19	0.40

[a] Porosity data of the silicas are obtained from mercury porosimetry.

repulsive interactions. A similar modification of the chain mobility in the vicinity of hard filler particles is found in polymer nanocomposites, where, depending on the compatibility, a positive or negative shift of the glass transition temperature might be observed in analogy to that in thin films[13−16] For attractive interactions, the small shift to higher glass transition temperatures can be accompanied by a broadening of the glass peak on the high-temperature side[15] or the shape of the corresponding step of the heat capacity obtained from DSC measurements exhibits a double structure, indicating an additional contribution on the high-temperature side.[16] Many silica-filled polymer systems, e.g., PDMS/fumed silica,[16] PDMS/in situ silica,[17] or various polymers filled with very fine silica,[18] exhibit two distinct glass transition temperatures, where the high-temperature peak is assigned to an interfacial layer of polymer segments with restricted mobility.

In the study of polymer−filler interactions in carbon black-filled and silica-filled rubbers low-resolution proton ^{1}H NMR has been used.[3,17,19−22] In all these studies, physical adsorption of rubber chains onto the surface of the filler is observed, causing significant immobilization of the polymer chains near the filler surface. This immobilization is in most cases interpreted as bound rubber resulting from interactions between the filler and the rubber. The immobilized bound rubber consists of two microshell regions with strongly differing local chain mobility: a tightly bound, low-mobility, almost rigid phase, which directly covers the filler surface, and a loosely bound, more mobile rubber phase remote from this interface. Grafting of silica in particular with methanol or hexadecanol was shown to decrease the ability of the filler to interact strongly with the surrounding rubber.[3,19−21] Thus, it appears that there is indeed some kind of attractive interaction between the highly polar silica surface and the typically nonpolar polymer chains.

In contrast to carbon black as reinforcing filler the hydrophily of silica is very high, and there is always some water adsorbed on the surface of the silica, which competes with the adsorption of the polymer chains.[16,17] Several authors[16,17,23,24] reported the identification of water by dielectric relaxation spectroscopy on the surface of pure silica as well as on the silica surface in polymer composites. But up to now, the influence of water on the polymer−filler interaction as well as the interaction with the used coupling agents is not well investigated, especially in practically relevant composites.

In the present paper, we will focus on the relaxation dynamics of adsorbed water at various silica surfaces in high-performance elastomer composites consisting of solution styrene−butadiene rubber (S-SBR) and precipitated silicas compounded under industry-like conditions. Different silicas with varying morphology and water content are investigated by dielectric spectroscopy, implying that water islands or complete coverage of the silica surface can be identified by the dielectric response. We will show that there is an adlayer of water on the silica surface in the presence of polymer with and without silane. The effect of silica type and coupling agent on the observed two low-temperature relaxation transitions will be discussed, showing that they can be interpreted as fluctuations of physically adsorbed water molecules and of hydroxyl groups, respectively.

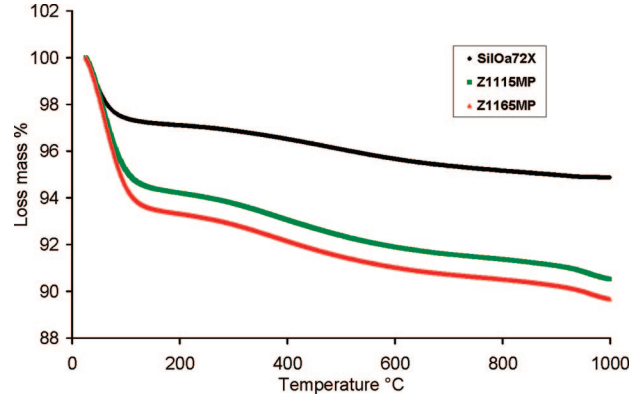

Figure 1. TGA measurements of the loss mass up to 1000 °C of three different silicas, as indicated.

Experimental Section

Samples have been prepared based on solution styrene−butadiene rubber (S-SBR) 5025-1 with 50 wt % vinyl and 25 wt % styrene groups and an oil content of 37.5 phr (parts per hundred rubber). A systematic variation of the filler has been performed varying the volume fraction, the type of precipitated silica, and the type of surface modification (silane) of the filler. The different precipitated silicas, provided by Rhodia, used in this study are highly dispersible silica (HDS) types (Z1115 MP, Z1165 MP, ZHRS 1200MP, Zeosil PREMIUM 200MP) and a silica with low silanol content (Siloa72X). They mainly differ in the water content and amount of silanol groups on the silica surface, the specific surface area, determined by N_2 adsorption, and in the porosity and pore distribution, obtained from mercury porosimetry. All characteristic properties of the investigated types of silica are summarized in Table 1. For the mercury porosimetry measurement, the contact angle was specified to 140°, the porous distribution width parameter, given in Table 1, was defined by the half-height width in nm divided by d_{max}. The total number of Si−OH/nm^2 is calculated from the loss ignition at 1000 °C as

$$nb_{SiOH}/nm^2 = \frac{[(IL - moisture)/100] \times (2/18) \times 6.0210^{23}}{\text{specified surface } N_2 \times 10^{18}}$$

The moisture, determined from the weight loss during tempering for 2 h at 105 °C, is also given in Table 1. It characterizes the water coverage of the silica surface, i.e., the amount of physically adsorbed water.

It is demonstrated in Figure 1 that the moisture content determined according to ISO from the water and ignition loss at 105 and 1000 °C, respectively, is in fair agreement with TGA measurements of the loss mass up to 1000 °C. Accordingly, the initial drop of the mass at temperatures up to about 150 °C indicates a moisture content of about 3% for Siloa72X and about 6% for Z1115Mp and Z1165MP. The final drop of the mass at 1000 °C delivers a loss ignition of about 5% for Siloa72X and about 9% and 10% for Z1115Mp and Z1165MP, respectively.

For mixing of the elastomer with the filler and the vulcanization chemicals (see Table 2) a tangential internal kneader was used (Haake mixer with a chamber capacity of 300 mL and a filling factor of 0.75). The silanization of the precipitated silica was

Table 2. Composition of the Base Mixture and Processing Conditions

component	amount	remarks
SBR	137.5	S-SBR (Buna VSL5025-1 from Lanxess) with a T_g value close to −20 °C; 100 phr of SBR extended with 37.5 ± 2.8% of oil
ZnO	2.5	
stearic acid	2.0	
antioxidant	1.9	*N*-1,3-dimethylbutyl-*N*-phenyl-*p*-phenylenediamine (Santoflex 6-PPD from Flexsys)
DPG	1.5	diphenylguanidine (Vulkacit D from Bayer)
CBS	2.0	*N*-cyclohexyl-2-benzothiazyl-sulfenamide (Rhenogran CBS-80 from Lanxess)
TBzTD	0.2	tetrabenzylthiuram disulfide (Perkacit TBzTD from Flexsys)
sulfur	1.1	
		Processing Conditions
	temp (°C)	ingredient
stage 1		
0′	80	SBR
1′30		2/3 silica + silane
3′		1/3 silica
5′		stearic acid
7′	155	dump
stage 2		
0′	80	master batch
1′		ZnO + antioxidant
4′	150	dump

Table 3. Composition of the Samples

sample name	filler	surface modification	filler amount (phr)
B	Z1165MP	TESPT (6.4 phr)	80
C	n.a.	n.a.	0
E	Z1115MP	TESPT (5.0 phr)	83
I	Z1165MP	TESPT (2.4 phr)	30
K	Z1165MP	TESPT (8.0 phr)	100
L	Z1165MP	OCTEO (6.6 phr)	80
M	Z1165MP	n.a.	80
AA	Siloa72X	n.a.	80
G	Zeosil PREMIUM 200MP	TESPT (7.4 phr)	74
H	ZHRS 1200MP	TESPT (5.8 phr)	58
U[a]	Z1165MP	n.a.	80
V[a]	Z1165MP	n.a.	80
W[a]	Z1165MP	n.a.	80

[a] For samples U, V, and W a variation of dispersion (mixing time) has been performed.

performed in situ in the internal kneader as a two-stage process at maximum temperatures of 155 °C, which is explicitly described in Table 2. The samples without silane were mixed in a one-step procedure with reduced mixing time.

The silanes used were the bifunctional coupling agent (bis(triethoxysilylpropyl) tetrasulfide (TESPT)), allowing for a sulfur-based chemical coupling to the polymer, and the monofunctional covering agent octyltriethoxysilane (OCTEO) without sulfur. The amount of silane was increased linear with the concentration and specific surface of silica as well as the functionality of silane to obtain a similar surface coverage with reactive units of the silane, i.e., about 1.1 active functional groups per nm^2 of the silica surface. This was focusing at a constant (chemical) coupling density of polymer chains at the silica surface independent of silica and silane type and silica concentration. The filler amount and the type of surface modification for the different samples are listed in Table 3. For the samples U, V, and W additionally a variation of dispersion has been performed by reducing the mixing time. The macrodispersion was estimated with a light microscopic techniques (DISPERGRADER) by measuring the relative area of nondispersed silica agglomerates.[25]

Circular specimens where prepared by compression-molding vulcanization at 160 °C in a special mold yielding four individual specimens with a thickness between 200 and 250 μm and a diameter of 43 mm. The achieved typical thickness variation over the diameter was less than 5%. Specimens not fulfilling this thickness variation limit were discarded. Vulcanization times were determined with a vulcameter (ODR Monsanto 100S-DIN 53529) measuring the time passed until 98% of the maximum torque had been achieved at 160 °C.

The measurement of the dielectric properties of the specimens was performed with a broadband dielectric spectrometer, BDS 40 system manufactured by Novocontrol GmbH, Germany, providing a frequency range from 3×10^{-5} to 1×10^{7} Hz. The measurements were performed in the frequency window from 0.1 Hz to 1 MHz over a temperature range from −100 to +100 °C. The temperature-control subset provided a temperature control better than 0.5 °C. The measured geometry was a disk shaped capacitor with a diameter of 40 mm. Thin gold layers were sputtered onto the flat surfaces of the specimens to ensure good electrical contact to the electrode plates. The specimens were placed between the two gold-plated brace electrodes of the test capacitor. Additionally, a force-limiting spring was used to ensure that always the same clamping force was exerted onto the test capacitor, keeping thickness and electrical contact as comparable between different samples as possible. The capacitor gap was maintained by the thickness of the rubber sample only.

Results

Figure 2 shows the dielectric loss, ε'', as a function of temperature and frequency in example for two different filled S-SBR (5025-1) samples. The spectra of both samples (Figure 2a,b) exhibit the well-defined dynamic glass process of the matrix. The strong increase of the dielectric loss at low frequencies and high temperatures is a typical observation and most likely caused/dominated by ion migration and electrode polarization effects and will not be discussed further in this paper.[26] Furthermore, both spectra possess well-developed relaxation processes at temperatures below the glass transition. They are associated with the presence of the silica particles in the polymer matrix. For the sake of simplicity, we will call these processes "silica process" or "silica peak" 1 and 2 (SP1 and SP2) as indicated in Figure 2a,b, where the SP1 is the process at lower temperatures.

Rubber−filler composites are heterogeneous, multicomponent systems prepared in a multistep mixing procedure. As the dielectric properties depend very sensitively on the geometry of the specimen, i.e., small inhomogeneities in the thickness of the test capacitor, the absolute value of the dielectric properties of systematically varied rubber−filler composites can differ. Figure 3a shows, as an example, the dielectric loss spectra of two compounds of identical composition (charge 1 and 2). ε'' is plotted as a function of temperature at a fixed frequency of 10^6 Hz, showing the glass transition and the "silica processes" in the accessible temperature range. The glass transition occurs at about 50 °C at 1 MHz for the S-SBR 5025-1. The relaxation process associated with the filler is located at about −60 °C. Between the two samples the peak amplitude differ by about 20%, probably due to an insufficient estimation of the sample thickness. To increase the sensitivity of the measurements, very thin samples of about 200 μm thickness were used, leading to pronounced effect on the loss peak amplitude even for small variations in the thickness of the samples. Using the height of the glass transition peak as an internal standard normalization shows the match of the dielectric behavior of the two samples (Figure 3b) throughout the measuring range. Thus, this procedure allows a relative comparison between different samples of identical composition as long as the "internal standard" remains unchanged.

Figure 4 shows the normalized dielectric loss, $\varepsilon''(T)$, at 10^6 Hz as a function of temperature for different concentrations of silica. With increasing filler volume fraction the silica peaks at temperatures of −60 to −70 °C are clearly increasing. The

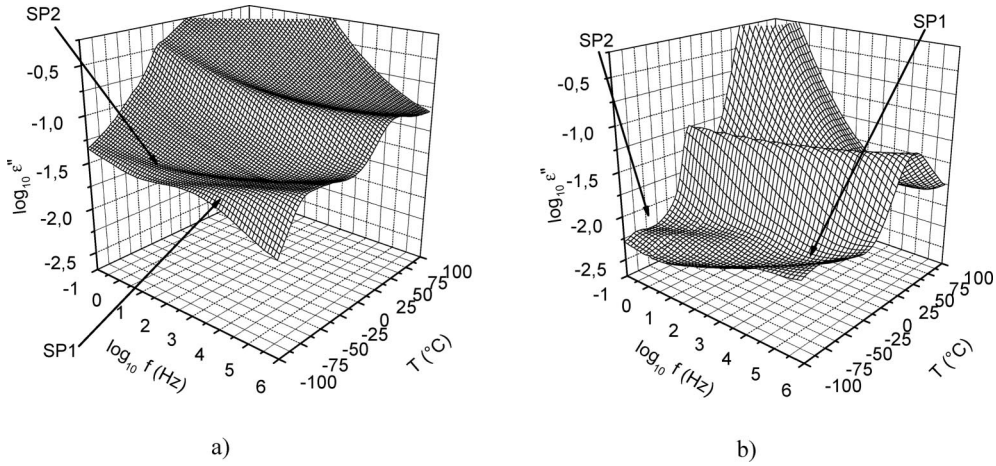

Figure 2. Dielectric loss vs temperature and frequency for (a) S-SBR 5025-1 filled with 80 phr of a high dispersible precipitated silica Z1165MP with surface modification by TESPT (sample B) and (b) S-SBR 5025-1 filled with 80 phr of a silica with low silanol and moisture content Siloa72X and without surface modification by silane (sample AA).

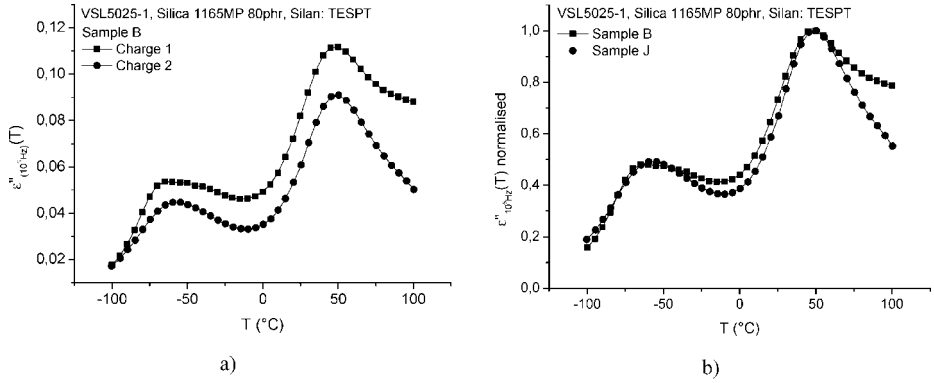

Figure 3. (a) Dielectric loss of two independently mixed samples B of identical composition (charge 1 and 2). (b) Normalization onto the peak maximum of the glass transition demonstrates almost identical dielectric behavior of the individual samples apart from some feature in the high-temperature region beyond the glass transition.

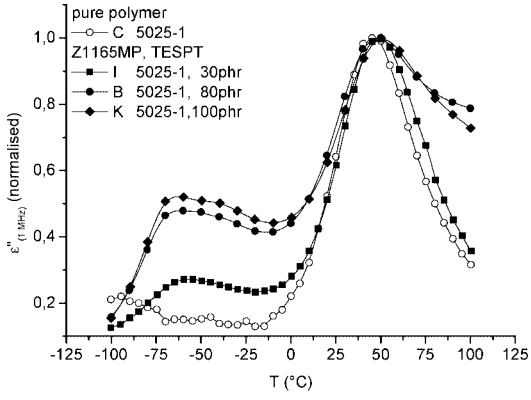

Figure 4. $\varepsilon''(T)$ at 10^6 Hz normalized with respect to the peak maximum of the glass transition for different samples of S-SBR 5025-1 with various concentrations of silica Z1165MP surface-modified with TESPT.

samples with higher silica content, 80 and 100 phr silica, exhibit the double-peak structure labeled with SP1 and SP2. Furthermore, a slight shift from ca. −60 °C for the 30 phr sample to ca. −70 °C for the samples with 80 and 100 phr silica content can be noticed. Unfortunately, the temperature dependence of the relaxation strength of both peaks shows no clear picture, which might be due to the limited experimental window. For most samples the relaxation strength of the peaks SP1 and SP2 increases with temperature, but SP1 of sample L and M show a clear decreasing temperature characteristic.

The pure polymer sample without silica shows a week β-process with activation energy of about 0.15 eV. We point out that this is much smaller than the activation energies of the two silica peaks (see below), indicating that fluctuations of side groups (vinyl, styrene) take place in the glassy state of the rubber matrix. Furthermore, we stress that the location of the glass transition process is not influenced by the addition of silica, which was also found in previous studies.[27,28] Instead, a broadening of the peak with increasing silica content is observed, only, which can be related to the slowed down dynamics of the chains in the vicinity of the filler particle surface.[12,13]

Figure 5 demonstrates the influence of the surface modification by silane on the amplitude of the silica peaks. It is interesting to note that only the amplitude of SP1 depends on the modification of the polar silica surface with nonpolar silane. Sample M without silanisation of the silica surface displays the highest peak amplitude corresponding to the highest dipole moment density in the sample series. For the silanized samples L and B the peak height diminishes with increasing functionality of the silane (OCTEO monofunctional and TESPT bifunctional) although the amount of silane was dosed equimolar according to the functionality of the silane and in the same proportion with respect to the silica. There is apparently no effect of the silanization on the intensity of the peak SP2 which does not change in height and as well stays at the same position.

In Figure 6 the change of the amplitude height of the silica peaks with different types of silica is demonstrated. The silicas differ in water content, surface area, and amount of silanol groups, as listed in Table 1. The amplitude height of the main

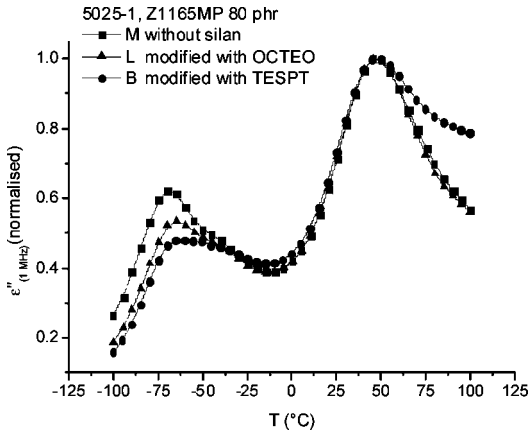

Figure 5. $\varepsilon''(T)$ at 10^6 Hz normalized with respect to the peak maximum of the glass transition for different samples of S-SBR 5025-1 with same concentrations of silica but with different surface modifications.

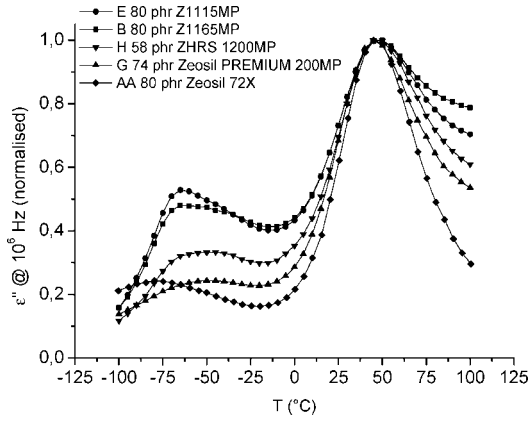

Figure 6. $\varepsilon''(T)$ at 10^6 Hz normalized with respect to the peak maximum of the glass transition for various samples of S-SBR 5025-1 filled with different types of silica.

peak SP1 is apparently decreasing with decreasing water content and amount of silanol groups. The silicas with the highest moisture and Si−OH content (Z 1115 MP (sample E), Z 1165 MP (sample B), and ZHRS 1200 MP (sample H)) show the most pronounced peak amplitude. The samples with the lowest peak amplitude (Zeosil 200 MP (sample G) and Siloa 72 X (sample AA)) correspond to the types of silica with the lowest concentration of OH groups as well as the lowest water content (cf. Table 1). The remarkable low amplitude of the silica peaks indicates a correlation between the silica peak height and the amount of water and/or the amount of silanol groups. Note that in Figure 6 only SP1 of sample AA and G is visible, since the SP2 peak is more separated from SP1 and hidden by the glass peak.

In Figure 7 three samples with the same composition but different dispersion states of the silica Z 1165 MP are compared to each other. The shape of the different loss curves does not change significantly with improved dispersion. As well, SP1 and SP2 can be identified in all dispersion levels, indicating that poor dispersion does not cause the existence of one or both silica peaks. Obviously, both peak amplitudes seem to be nearly independent of the dispersion state, indicating that the relaxation strength is not affected by the amount of polymer−filler interface, which should be higher in a well-dispersed state.

For a quantitative evaluation of the dielectric spectra the empirical Cole−Cole function (1) has been fitted to the data allowing the deduction of activation energy diagrams for the different processes, causing the silica peaks SP1 and SP2. ε' and ε'' have been fitted simultaneously.

$$\varepsilon(\omega) = \varepsilon_\infty + \sum_j \frac{\Delta\varepsilon_j}{1 + (i\omega\tau_j)^{\alpha_j}} \quad \text{with } \tau = \frac{1}{\omega} = \frac{1}{2\pi f} \tag{1}$$

The activation energies of the individual processes have been obtained by fitting the data with eq 1, resulting in the characteristic relaxation frequency, f_j, of the considered process. In a representation of f_j against the reciprocal temperature, $1/T$, the resulting linear behavior can be described by the Arrhenius equation:

$$\log f_{SP} = \log f_\infty - \frac{E_a}{k_B T} \log e \tag{2}$$

The results of this procedure are shown in Figure 8, and the fit parameters are summarized in Table 4.

In Figure 8a the silica process 1 (SP1) is observed in the same temperature and frequency range for all samples. For the silica Z 1165 MP without modification in S-SBR 5025-1 (sample M) an activation energy of 0.6 eV is obtained, which correlates to the activation energy of ice-like water clusters.[29,30] With modification of the same silica with TESPT (sample B) in the rubber matrix an increase of the activation energy to 0.69 eV is detectable. In samples B and E, with the same filler content and silane modification but with different types of silica, the values vary only slightly around 0.67 eV, but the content of moisture of both types of silica is only slightly differing between 6.1% and 6.5%. For the sample AA with very low water content and amount of silanol groups the activation energy in S-SBR 5025-1 lies with around 0.4 eV, significantly lower than in the other samples. This is similar for the sample G with 0.5 eV, which as well has a low water content and amount of silanol groups. It can be stated that the activation is increasing with increasing moisture content and amount of silanol groups. In addition, silanization implies a hydrophobization of the silica surface and hence a stronger polymer−filler interaction. This results in an increasing activation energy of the silica peak SP1. For the pure silica Z 1165 MP an activation energy of 0.46 eV is obtained, which is significantly smaller than that of the corresponding composites B, L, and M. This indicates that the presence of polymer or silane at the silica surface reduces the mobility of the hydration water.

In the samples E, B, M, and H the silica process 2 (SP2) is found in the close vicinity to SP1 but is distinguished from SP1 by a stronger temperature dependence (Figure 8b). The activation energies of these samples have almost identical values of nearly 1 eV independent of the amount of silica, silica type, or surface modification. The water content of these samples differs only slightly between 6.1% and 6.7%. On the other hand, the SP2 of the samples AA and G with lower water content and less silanol groups occurs at significant higher temperatures and

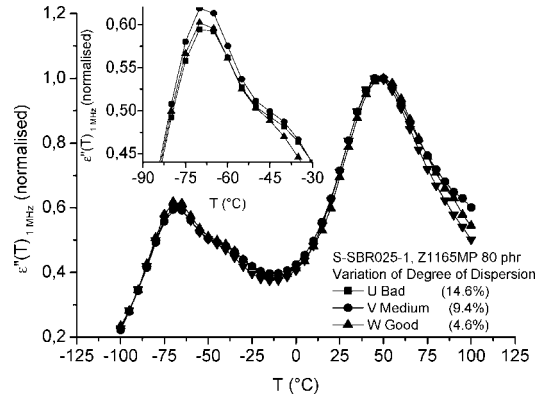

Figure 7. $\varepsilon''(T)$ at 10^6 Hz normalized with respect to the peak maximum of the glass transition for different samples of S-SBR 5025-1 with same composition but different dispersion states.

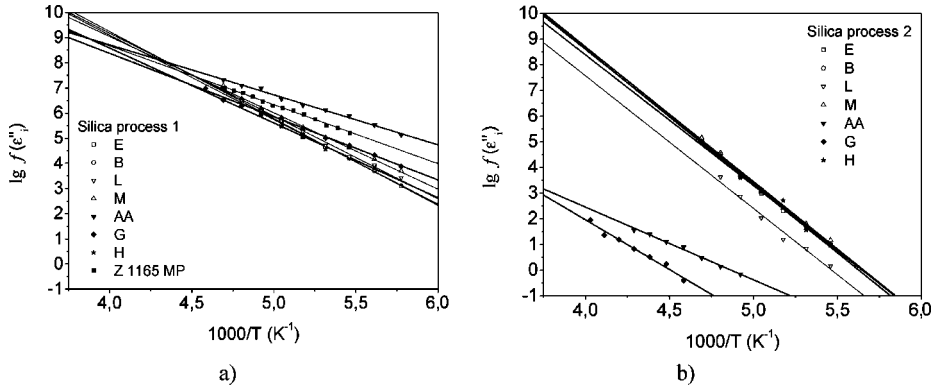

Figure 8. Activation diagrams of the silica process 1 (a) and silica process 2 (b) of the different samples. The silica process 1 for the pure silica Z 1165 MP is also shown for comparison reasons. The lines are fits according to eq 2.

Table 4. Activation Energies and Front Factors of the Fits in Figure 8 According to Eq 2 and Water Coverage, Θ, According to Eq 3 with Moisture *h* and Specific Surface $S_{specific}$ Taken from Table 1

	silica process 1		silica process 2		
sample	log f_∞	E_a/eV	log f_∞	E_a/eV	Θ
E	22.53 ± 0.70	0.666 ± 0.027	29.05 ± 0.85	1.021 ± 0.032	1.73
B	23.06 ± 0.30	0.686 ± 0.011	28.72 ± 0.26	1.009 ± 0.010	1.13
L	22.34 ± 0.46	0.653 ± 0.017	28.21 ± 1.47	1.020 ± 0.055	1.13
M	21.18 ± 0.33	0.602 ± 0.013	29.69 ± 0.89	1.041 ± 0.035	1.13
AA	16.65 ± 0.34	0.394 ± 0.013	13.77 ± 0.51	0.561 ± 0.022	0.53
G	18.43 ± 0.28	0.499 ± 0.011	17.44 ± 1.06	0.768 ± 0.049	0.74
H	20.48 ± 0.80	0.590 ± 0.030	29.43 ± 1.24	1.034 ± 0.049	1.01
Z 1165MP	18.01 ± 0.35	0.464 ± 0.014	–	–	1.13

lower frequencies than in the other samples and displays a substantially lower activation energy. The difference of the activation energy of SP2 between sample AA and G correlates roughly with the total number of surface silanol groups per nm^2, which was found to be 7.6 and 8.4 per nm^2, respectively, but also with the moisture content with 3.1 and 5.4 wt % (cf. Table 1). On the other hand, the activation energy of sample G and sample E is quite different although the water content is comparable. However, the total number of silanol groups per nm^2 is much larger for the sample E. For the pure silica Z 1165 MP the relaxation process SP2 could not be observed.

The observed different dielectric behavior of SP1 and SP2 suggests that beside the water content and the number of silanol groups the differences in the surface area between the silica types have to be taken into account. An important quantity, which could relate the differences in the dielectric properties between the samples, is the surface coverage, Θ, i.e., the number of monolayers of adsorbed water. The water content necessary to obtain a complete monolayer of water on the silica surface, $\Theta = 1$ can be calculated from the specific surface area, $S_{specific}$, of the silica listed in Table 1. By assuming a hexagonal arrangement of the water molecules on the surface with a lattice constant of $d = 3.2$ Å, corresponding to the size of the water molecules, the monolayer capacitance h_{mono} can be estimated by eq 3:[23]

$$\Theta = \frac{h}{h_{mono}}, \quad \text{with } h_{mono} = S_{specific}\frac{2}{\sqrt{3}d^2}\frac{M_{H_2O}}{N_A} \tag{3}$$

Here, h is the moisture, M_{H_2O} is the molar mass of water, and N_A is Avogadro's number. According to eq 3, the monolayer capacitance h_{mono} amounts to 3.7 wt % for Z1115MP, 5.4 wt % for Z1165MP, 5.9 wt % for Siloa72X, 7.3 wt % for Zeosil PREMIUM 200MP, and 6.6 wt % for ZHRS 1200MP. Then, the moisture content of the silicas listed in Table 1 can also be expressed by the coverage Θ. These values are listed in the right column of Table 4.

In Figure 9 the activation energies of SP1 and SP2 are plotted against the water coverage Θ. This demonstrates that the activation energy for both of the relaxation transition, SP1 and SP2, increases first with hydration level. However, the samples with at least one monolayer of water ($\Theta > 1$) exhibit almost the same activation energy; i.e., sample H with about one monolayer of water exhibits the same behavior as the samples E, B, and M. For the other two samples AA and G, with less than one monolayer of water adsorbed on the silica surface, the activation energy increases almost linear with the hydration level. This is indicating a connection of the silica peaks SP1 and SP2 with the water coverage on the silica surface. Note that the density of silanol groups also varies with the amount of adsorbed water, which amounted to 11.3 silanol groups per nm^2 for silica ZHRS 1200MP (sample H). However, this is still significantly lower than the values of 21.3 and 15.1 nm^{-2} for the silicas of samples E, B, and M (cf. Table 1).

Discussion

Zhuralev describes the hydroxylation states of amorphous silicas depending on pretreatments.[31] The surface silanol groups of the silica constitute the first layer. The amount of surface silanol groups and fractions of siloxane, isolated, geminal, and vicinal silanols depend only on the preconditions. Layers of physically adsorbed water are bound by hydrogen bridges interacting with the silanol groups. Thus, we attribute the existence of the two distinct relaxation processes to the fluctuations of surface silanol groups and to the hydration shell of physically adsorbed water on the silica surface. Similar results on the dielectric response of adsorbed or confined water have been reported in systems of vermiculite clay,[32,33] of mesoporous MCM-41 molecular sieves,[23] of silica gels,[34] of Aerosil (11), and of Vycor glass.[29,35,36]

Let us first discuss the relaxation process SP1. The activation energy of this relaxation process varies only slightly for the samples with at least one monolayer of physically adsorbed water (samples E, B, M, and H) at about 0.6 eV. This corresponds to the activation energy of water fluctuations in ice with three hydrogen bonds per water molecule.[29,30] The location of this relaxation transition as well as the obtained

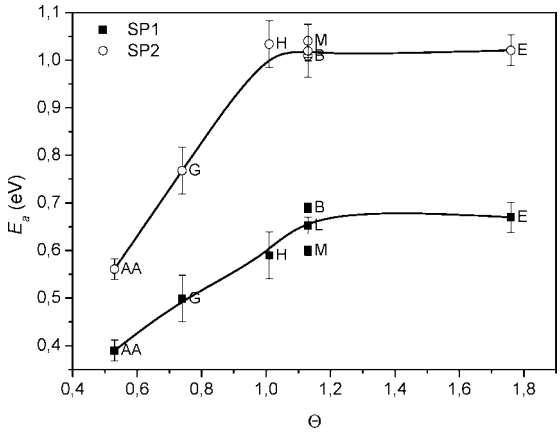

Figure 9. Relation between water coverage and activation energy for SP1 and SP2 (lines are guides for the eyes).

activation energy is in agreement with the findings of several other authors[17,23,24] for water fluctuations in samples with sufficient high humidity. We therefore attribute SP1 to physically adsorbed hydration water and SP2 to fluctuations of the silanol groups at the surface of the silicas. The significantly lower content of physically adsorbed water in samples AA and G does not principally alter the dynamic signature of the dielectric response. Hence, SP1 of these samples is observed in the same frequency−temperature range as the one of the fully hydrated samples. Nevertheless, the activation energy for these samples is significantly lower at 0.4 and 0.5 eV, respectively, corresponding to more mobile fluctuating water molecules. With increasing hydration level an increase of the activation energy is observed, which can be attributed to a reduction in the mobility of the water molecules due to an increasing number of hydrogen bridging partners. For the pure silica Z 1165 MP the activation energy of 0.46 eV corresponds well to a single monolayer of water with about 2.3 hydrogen bridging per water molecule. The activation energy increases up to 0.6 eV when the same silica is dispersed in a polymer matrix (sample M), indicating that the immobilized glassy polymer chains hinder the mobility of the fluctuating water molecules significantly. In this context we note that the pre-exponential front factors f_∞ listed in Table 4 are quite high and apparently in contradiction to localized relaxation processes. However, as reported by Cerveny et al.,[24] a crossover to lower activation energies will probably appear at temperatures above the glass transition of the matrix because the much higher mobility of the polymer chains above $T_g \approx -10$ °C will also increase the mobility of the hydration water. This crossover is expected to take place at higher frequencies in the gigahertz range. Accordingly, the pre-exponential front factor f_∞ of the samples cannot be identified with a physically reasonable jump rate.

The surface modification with silane causes a decrease of the amplitude of the silica process 1 (cf. samples M with B) which is shown explicitly in Figure 5. The substitution of water bound at surface hydroxyl groups by nonpolar TESPT/OCTEO renders the interpretation of a reduced dipole moment density associated with SP1. This indicates that due to hydrophobization by the coupling agents a part of the water is migrating into the polymer. During the complicated multistep mixing procedure at high temperatures of 150 °C, where the silanization reaction takes place (cf. Table 2), this water can evaporate more easily due to the weaker interaction with the silica surface, resulting in a less pronounced peak SP1. A comparison of samples B and M in Table 4 demonstrates that the activation energy increases by silanization with the chemical coupling agent TESPT from 0.6 to 0.69 eV. Furthermore, sample L modified with the covering agent OCTEO, without sulfur functions,

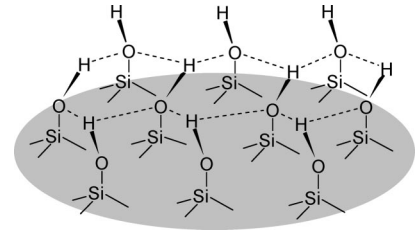

Figure 10. Sketch of a strongly "chemisorbed water layer" formed by the clustering of silanol groups via hydrogen bridges. Geminal and isolated silanol groups have been omitted for the sake of clarity (after ref 37).

exhibits an intermediate activation energy of 0.65 eV. This indicates that the hydrophobization and chemical coupling of the polymer chains to the silica surface reduces the mobility of the remaining hydration water on the silica surface. Thus far, the activation energy reflects the coupling strength of the polymer chains to the silica surface and allows for a prediction of the polymer−filler interaction strength of the composites.

In contrast to SP1, SP2 exhibits a distinct dynamic signature in dependence of the existence of a complete layer of physically adsorbed water. According to the Zhuralev model, precipitated silicas have a constant surface silanol concentration independent of the content of physically adsorbed water. Agamalian et al.[37] have shown in their neutron diffraction experiments on Vycor glass that there is an interaction of the hydroxyl groups on the silica surface due to the formation of hydrogen bridges. The silanol groups are organized in patches or islands of 40−60 molecules connected to each other by hydrogen bonds forming ordered arrays of water molecules on the silica surfaces, also existing in pyrogenated silicas, coexisting with more spaciously distributed individual molecules or groups of several molecules (Figure 10).

In the case of hydration levels $h \geq h_{mono}$ ($\Theta \geq 1$), an identical dielectric response for the different samples is observed with an activation energy of about 1 eV (samples E, B, M, and H). This activation energy is very high due to the high hindrance of the silanol groups interacting with each other and additionally covered with a monolayer of water. As well, the relaxation rates of these samples do not show any difference. The energetic environment of the surface hydroxyl groups is therefore very similar for the different samples. In the case of $h < h_{mono}$, the relaxation process is about 3−4 orders of magnitude slower and occurs at higher temperatures (samples AA and G). Nevertheless, the activation energy is significantly lower at 0.56 and 0.78 eV, respectively. The lower activation energy of these samples with a lower hydration level as well as smaller amount of silanol groups can be explained with a lower number of interacting hydrogen bonds due to the reduced number of water molecules and silanol groups available per unit surface area.

After all, there remains an open questions concerning the relaxation transition SP2 that cannot be explained by the above interpretation. The amplitude of SP2 is not changing with surface modification (cf. Figure 5). Accordingly, the number of reactive silanol groups per surface unit should be equal for the samples with and without silane, which appears unlikely. From this observation one might conclude that SP2 of the samples E, B, M, and H with the very high activation energy of about 1 eV is not related to the relaxation of hydroxyl groups but results from another process, which does not appear for the samples AA and G with low hydration level. This seems reasonable, since the relatively weak relaxation process of hydroxyl groups of the samples AA and G becomes visible only due to the low amplitude of SP1 for these samples (cf. Figure 2). Accordingly, the relaxation process of hydroxyl groups of the samples E, B, M, and H should have a low relaxation strength as well and

could therefore be hidden by the large relaxation strength of SP1. Nevertheless, the origin of the observed secondary relaxation transition for the samples E, B, M, and H with the activation energy of 1 eV remains unclear. A possible explanation could be strongly confined hydration water in silica pores, but no clear correlations with the parameters characterizing the porosity (cf. Table 1) can be obtained. Therefore, we have to leave this question open for future investigations.

Conclusions

The dynamics of physically adsorbed water at the silica interface of elastomer composites filled with various types of silica with and without coupling agent silane has been investigate giving some more inside into the mechanisms of polymer−filler interaction in silica filled elastomer systems. In particular, the following conclusions can be drawn:

i. The amount of hydration water on the silica surface of high-performance elastomer composites can be detected by dielectric spectroscopy. It is found to be related to the main relaxation peak SP1, showing an increase of the intensity with the amount of silica (Figure 4) and a connection between the content of hydration water of the silica and the peak intensity (Figure 6).

ii. Since the silica peak SP1 is increasing with the moisture content but as well is dependent on the surface area, the most significant information can be obtained with the surface coverage $\Theta = h/h_{mono}$. For hydration levels $h < h_{mono}$ ($\Theta < 1$), the activation energy increases successively with h. For the silica with the lowest moisture content, the activation energy is low (~0.4 eV), since the mean number of hydrogen bonds is low (about two) and the water molecules on the silica surface can fluctuate more mobile. In the case of silicas with the higher moisture content ($\Theta \geq 1$), the activation energy is significantly higher (~0.6 eV), corresponding to a larger mean number of hydrogen bonds (about three), and no changes in the activation energy are found (cf. Figure 9). This can be attributed to an increasing hindrance of the water mobility due to the increasing amount of hydrogen bridges, resulting in a complete change of the water surrounding structure to ice-like water clusters.

iii. The modification of the silica surface by a coupling agent reduces the intensity of SP1 due to the substitution of water molecules and a probable migration and evaporation of water in the polymer matrix (Figure 5). The activation energy increases by silanization with TESPT from 0.6 to 0.69 eV, indicating that hydrophobization and chemical coupling of the polymer chains to the silica surface reduces the mobility of the hydration water. Modification with the covering agent OCTEO, without chemical coupling functionalities, exhibits an intermediate activation energy of 0.65 eV. This opens the possibility to assess and predict the polymer−filler interaction strength of high-performance silica filled elastomers by measuring the activation energy of the hydration water of the composites.

iv. The subsidiary relaxation peak SP2 has partly be related to fluctuations of silanol groups. A complete understanding of this relaxation transition could not be achieved and requires more investigations.

As dielectric spectroscopy detects selectively effects on the silica surface and its close surrounding, this easy to use technique can be employed as a tool to examine the extent of hydroxylation and silanization of surfaces of reinforcing silicas in rubber compounds as well as the extent of hydration of silica surface. It has been shown that dielectric spectroscopy can distinguish between complete and incomplete coverage of the silica surface with water. As it has been evidenced that there is a substantial coverage of the silica surface with water in silica−rubber compounds prepared under industrial-like conditions, it raises again the question on the nature of the attractive polymer−silica interaction.

References and Notes

(1) Wolff, S. In *Silica Based Tread Compounds—Background and Performance*; Tire Tech93: Basel, Switzerland, 1993.
(2) Wang, M. J.; Wolff, S.; Donnet, J. B. *Rubber Chem. Technol.* **1991**, *64* (4), 559–576.
(3) Ou, Y. C.; Yu, Z. Z.; Vidal, A.; Donnet, J. B. *J. Appl. Polym. Sci.* **1996**, *59* (8), 1321–1328.
(4) Alberola, N. D.; Benzarti, K.; Bas, C.; Bomal, Y. *Polym. Compos.* **2001**, *22* (2), 312–325.
(5) Ou, Y. C.; Yu, Z. Z.; Vidal, A.; Donnet, J. B. *Rubber Chem. Technol.* **1994**, *67* (5), 834–844.
(6) Wolff, S.; Wang, M. J.; Tan, E. H. *Kautsch. Gummi Kunstst.* **1994**, *47* (2), 102–107.
(7) Wolff, S.; Wang, M. J. *Rubber Chem. Technol.* **1992**, *65* (2), 329–342.
(8) Hartmann, L.; Fukao, K.; Kremer, F. Molecular Dynamics in Thin Polymer Films In *Broadband Dielectric Spectroscopy*; Kremer, F., Schönhals, A., Eds.; Springer: Berlin, 2003.
(9) Grohens, Y.; Hamon, L.; Reiter, G.; Soldera, A.; Holl, Y. *Eur. Phys. J. E* **2002**, *8* (2), 217–224.
(10) Kremer, F.; Huwe, A.; Schönhals, A.; Rozanski, S. A. Molecular Dynamics in Confining Space In *Broadband Dielectric Spectroscopy*; Kremer, F., Schönhals, A., Eds.; Springer: Berlin, 2003.
(11) Forrest, J. A.; DalnokiVeress, K.; Stevens, J. R.; Dutcher, J. R. *Phys. Rev. Lett.* **1996**, *77* (10), 2002–2005.
(12) Long, D.; Lequeux, F. *Eur. Phys. J. E* **2001**, *4* (3), 371–387.
(13) Starr, F. W.; Schrøder, T. B.; Glotzer, S. C. *Macromolecules* **2002**, *35* (11), 4481–4492.
(14) Ash, B. J.; Siegel, R. W.; Schadler, L. S. *J. Polym. Sci., Part B: Polym. Phys.* **2004**, *42* (23), 4371–4383.
(15) Winberg, P.; Eldrup, M.; Maurer, F. H. J. *Polymer* **2004**, *45* (24), 8253–8264.
(16) Fragiadakis, D.; Pissis, P.; Bokobza, L. *Polymer* **2005**, *46* (16), 6001–6008.
(17) Kirst, K. U.; Kremer, F.; Litvinov, V. M. *Macromolecules* **1993**, *26* (5), 975–980.
(18) Tsagaropoulos, G.; Eisenberg, A. *Macromolecules* **1995**, *28* (18), 6067–6077.
(19) Berriot, J.; Lequeux, F.; Monnerie, L.; Montes, H.; Long, D.; Sotta, P. *J. Non-Cryst. Solids* **2002**, *307*, 719–724.
(20) Legrand, A. P.; Lecomte, N.; Vidal, A.; Haidar, B.; Papirer, E. *J. Appl. Polym. Sci.* **1992**, *46* (12), 2223–2232.
(21) ten Brinke, J. W.; Litvinov, V. M.; Wijnhoven, J. E. G. J.; Noordermeer, J. W. M. *Macromolecules* **2002**, *35* (27), 10026–10037.
(22) Litvinov, V. M.; Spiess, H. W. *Makromol. Chem.* **1991**, *192* (12), 3005–3019.
(23) Spanoudaki, A.; Albela, B.; Bonneviot, L.; Peyrard, M. *Eur. Phys. J. E* **2005**, *17* (1), 21–27.
(24) Cerveny, S.; Colmenero, J.; Alegria, A. *Eur. Phys. J. Spec. Top.* **2007**, *141*, 49–52.
(25) Putman, M.; Welsh, F. Dispersion Measurements Using Video Techniques. *Rubber World* **2005**, 21–26.
(26) Schönhals, A.; Kremer, F. Analysis of Dielectric Spectra In *Broadband Dielectric Spectroscopy*; Kremer, F., Schönhals, A., Eds.; Springer: Berlin, 2003.
(27) Fritzsche, J.; Klüppel, M. *Macromol. Rapid Commun.*, submitted.
(28) Le Gal, A. Ph.D Thesis, Leibnitz University, Hannover, **2007**.
(29) Gutina, A.; Axelrod, E.; Puzenko, A.; Rysiakiewicz-Pasek, E.; Kozlovich, N.; Feldman, Y. *J. Non-Cryst. Solids* **1998**, 235–237, 302−307.
(30) Hasted, J. B. *Aqueous Dielectrics*; Chapman and Hall: London, 1973.
(31) Zhuravlev, L. T. *Colloids Surf., A* **2000**, *173* (1−3), 1–38.
(32) Bergman, R.; Swenson, J. *Nature (London)* **2000**, *403* (6767), 283–286.
(33) Bergman, R.; Swenson, J.; Borjesson, L.; Jacobsson, P. *J. Chem. Phys.* **2000**, *113* (1), 357–363.
(34) Saraidarov, T.; Axelrod, E.; Feldman, Y.; Reisfeld, R. *Chem. Phys. Lett.* **2000**, *324* (1−3), 7–14.
(35) Puzenko, A.; Kozlovich, N.; Gutina, A.; Feldman, Y. *Phys. Rev. B* **1999**, *60* (20), 14348–14359.
(36) Ryabov, Y.; Gutina, A.; Arkhipov, V.; Feldman, Y. *J. Phys. Chem. B* **2001**, *105* (9), 1845–1850.
(37) Agamalian, M.; Drake, J. M.; Sinha, S. K.; Axe, J. D. *Phys. Rev. E* **1997**, *55* (3), 3021.

MA802002S